J|A|C|S COMMUNICATIONS

Published on Web 10/20/2009

Water Oxidation at a Tetraruthenate Core Stabilized by Polyoxometalate Ligands: Experimental and Computational Evidence To Trace the Competent Intermediates

Andrea Sartorel,[†] Pere Miró,[‡] Enrico Salvadori,[†] Sophie Romain,[‡] Mauro Carraro,[†] Gianfranco Scorrano,[†] Marilena Di Valentin,[†] Antoni Llobet,*[,‡] Carles Bo,*[,‡,§] and Marcella Bonchio*[,†]

ITM-CNR and Department of Chemical Sciences, University of Padova, via F. Marzolo 1, 35131 Padova, Italy, Institut Català d'Investigació Química (ICIQ), Av. Països Catalans 16, 43007 Tarragona, Spain, and Universitat Rovira i Virgili (URV), Marcel·lí Domingo s/n, Tarragona, Spain

Received June 19, 2009; E-mail: allobet@iciq.es; cbo@iciq.es; marcella.bonchio@unipd.it

Stabilization of adjacent transition metal centers through multiple-μ-hydroxo/oxo bridging units, is a powerful strategy adopted by Nature to effect multiple/cascade transformations.[1] In particular, the photosynthetic conversion of water into dioxygen is performed by photosystem II, using a polynuclear metal cluster, with four manganese and one calcium atom (Mn_4Ca).[2] The natural oxygen evolving complex (OEC) is able to mediate the required four-electron-four-proton process while undergoing a stepwise oxidation to a series of states S_i ($i = 0-4$), whereby the substrate waters are proposed to react when bound as terminal ligands.[3] The design of synthetic mimics capable of water oxidation in aqueous solution poses a formidable challenge.[4,5] In this quest, ruthenium complexes occupy a prominent role.[6] Among them, Meyer's "blue dimer", *cis*,*cis*-$[(bpy)_2(H_2O)Ru^{III}ORu^{III}(H_2O)(bpy)_2]^{4+}$ (bpy= 2,2′-bipyridine), was the first one described in literature.[7] Catalyst activation in vitro is achieved electrochemically or in the presence of a bulk oxidant as Ce^{IV}.[5d,7] However, because of a competing anation process, it deactivates after a few turnovers. Improvement of this system has been based on the use of a nitrogen-rich set of dinucleating ligands placing two ruthenium atoms in close proximity and in adequate orientation for catalysis.[8]

A recent breakthrough in the field is the innovative adoption of a totally inorganic and robust ligand system, taken from the polyoxometalate (POM) pool.[9,10] We have contributed by devising a straightforward, and high yield, protocol for the embedding of a catalytically active, tetraruthenium(IV)-μ-oxo core by two divacant γ-decatungstosilicate ligands, γ-$SiW_{10}O_{36}^{8-}$ (**SiW_{10}**). The resulting complex, $M_{10}[Ru_4(H_2O)_4(\mu\text{-}O)_4(\mu\text{-}OH)_2(\gamma\text{-}SiW_{10}O_{36})_2]$ (M_{10}**1**, M = Cs, Li), obtained in >80% yield, has been characterized in the solid state and in solution by multiple techniques.[9] Water oxidation catalyzed by **1** occurs in the presence of an excess of Ce(IV) with high turnover frequencies (>450 cycles·h^{-1}) and no deactivation.[5d,9] In this chemistry the kinetics are first-order with regard to the catalyst concentration, thus suggesting that the four-ruthenium core can master the mechanistic complexity expected for oxygen evolution, in an autarchy regime.[9] The four $Ru^{IV}-H_2O$ groups, within the catalyst core, are thus able to mediate the $4e^-/4H^+$ overall process by accessing such a multielectron catalysis, through sequential electron and proton loss, in a relatively narrow potential range (redox potential leveling).[11,12]

We report herein a combined investigation, addressing the evolution of **1** to high-valent intermediates, by means of Cyclic Voltammetry (CV), UV−vis, rRaman (rR), Electron Paramagnetic Resonance (EPR), and DFT calculations. In analogy with the natural enzyme,[3] five different oxidation states, generated from **1**, have been found to power the catalytic cycle for water oxidation (Scheme 1).

Scheme 1. Stepwise Transformation of the POM-Embedded Ru_4 Core in **1**, along the S_0-S_4 Oxidation States, under Oxygen Evolving Catalysis[a]

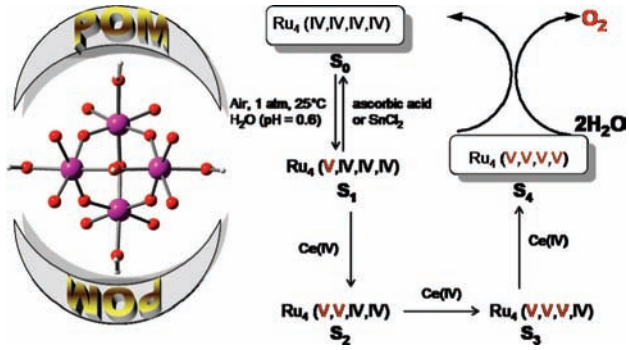

[a] The structure of the POM ligand is omitted for clarity reasons (see the Supporting Information for the complete structure).

The CV, performed for Li_{10}**1** (1 mM in H_2O, pH = 0.6) under anaerobic conditions, shows four anodic and three cathodic waves in a potential range from 0.35 to 1.15 V (vs SSCE). Three nearly reversible redox couples are observed at $E_{1/2}$ = +0.48, +0.61, +0.86 V with a peak separation of ΔE_p ($= E_{pa} - E_{pc}$) of 80, 60, 120 mV, respectively, corresponding to one-electron oxidations. The last anodic wave is observed at E_{pa} = +1.06 V (Figure S1). The electrochemical analysis points to a stepwise transformation of the Ru_4 core, involving the Ru_4{IV,IV,IV,IV} starting state, (**S_0**), and ultimately yielding a high valent, reactive, state (**S_4**) ascribable to Ru_4{V,V,V,V} (*vide infra*). The latter is the competent OEC, as electrocatalytic oxygen evolution is observed at E = 1.15 V (Figure S2). A four-step oxidation is also apparent from UV−vis spectrophotometric experiments, by monitoring the evolution of the absorption maximum at λ_{max} = 443 nm, in water at pH = 0.6, upon oxidation of **1**. While no significant λ_{max} shift is observed, the plot of A^{443} as a function of sequential one-electron titration yields a segmented line with four distinct slope changes (Figure 1; full spectra are reported in Figure S3).

Along the $4e^-/4H^+$ oxidative pathway, the first step leading to the **S_1** state, Ru_4{V,IV,IV,IV}, is readily accessed by aerial oxidation of **1** in water at pH = 0.6 (Scheme 1). Indeed, aerobic oxidation of diamagnetic **1** yields a paramagnetic species, as monitored by cryo-EPR, showing the formation of a broad rhombic signal (Inset in Figure 1). Spectral simulations provide a good description of the three main spectral components, with g_X, g_Y, and

[†] ITM-CNR and University of Padova.
[‡] Institut Català d'Investigació Química (ICIQ), Tarragona.
[§] Universitat Rovira i Virgili (URV), Tarragona.

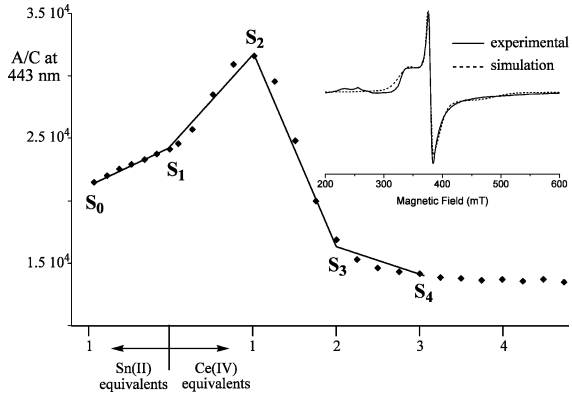

Figure 1. UV−vis spectrophotometric monitoring of A^{443} variation, normalized by concentration, of **1** (10^{-5} M) in H_2O (pH = 0.6), through $\mathbf{S_0}$−$\mathbf{S_4}$ states (see Scheme 1): $\mathbf{S_0}$ generated by addition of $SnCl_2$ to $\mathbf{S_1}$ (1 equiv); $\mathbf{S_1}$, resting state under aerobic conditions; $\mathbf{S_2}$−$\mathbf{S_4}$, generated by addition of 1−3 equiv of Ce(IV) to $\mathbf{S_1}$. Inset: experimental and simulated X-band EPR spectrum of the $\mathbf{S_1}$ state (1 mM in H_2O/ H_2SO_4, pH = 0.6), at 10 K.

g_Z values of 1.97, 1.67, and 1.43. This is in agreement with a metal-centered $S_{eff} = {}^1/_2$ ground state, thus identifying a Ru(V) species.[13−15] Noteworthy, restoration of diamagnetic **1** occurs by addition of 1 equiv of ascorbic acid or $SnCl_2$, as confirmed by the quantitative abatement of the EPR signal and by rR studies (*vide infra*).

The electronic and structural modification of **1** as a result of sequential electron/proton loss has been further addressed by rR spectroscopy and DFT calculations. The rR features, in the range 250−600 cm^{-1}, provide a sensitive tool to pinpoint the redox evolution of the Ru_4 core (Figure 2, Figure S4). To this aim, band deconvolution analysis has been associated with DFT computation of the vibrational frequencies of $[Ru_4(H_2O)_4(\mu\text{-}OH)_2(\mu\text{-}O)_4Cl_8]^{2-}$. Such calculations were not possible for the entire molecule; instead the tetraruthenate core capped with eight chloride atoms replacing the POM ligands was considered. This model for **1** was proven reliable by direct comparison of the calculated vs experimental UV−vis spectra, indicating an optimal matching of the electronic properties (see Figure S5).[16] According to calculations, the low wavenumber rR bands are assigned to Ru−(OH_2) stretching modes (250−400 cm^{-1}), while the prominent feature, at 456 cm^{-1}, is associated with vibrations of the Ru_4-core (Figures 2a and S6−S7). Upon oxidation of **1**, this latter band undergoes significant broadening, with the build up of new components at wavenumbers >500 cm^{-1} (Figure 2b−d). Noteworthy, no bands are observed in the region 750−850 cm^{-1}, thus ruling out the formation of Ru-oxo groups (Figure S4 in the Supporting Information).[15] On the contrary, the conversion of each pristine Ru(IV)−OH_2 to a Ru(V)−OH function may be envisaged, by the release of one single proton coupled to one-electron oxidation. Indeed, the calculated Raman modes of the *bis*-Ru(V)-hydroxo model, $[Ru^V_2(OH)_2Ru^{IV}_2(H_2O)_2(\mu\text{-}OH)_2(\mu\text{-}O)_4Cl_8]^{2-}$, predict the appearance of Ru−OH absorptions at >500 cm^{-1} (see the calculated modes at 577 and 595 cm^{-1}, Figures S8−S9). Such combined computational/experimental evidence is instrumental to address the structure of postulated intermediates $\mathbf{S_1}$−$\mathbf{S_4}$, generated from **1**, within the ruthenium-based OEC manifold. Accordingly, the $\mathbf{S_1}$ state is associated with $[Ru^V(OH)\text{-}Ru^{IV}_3(H_2O)_3(\mu\text{-}O)_4(\mu\text{-}OH)_2(\gamma\text{-}SiW_{10}O_{36})_2]^{10-}$, **2**, featuring a *mono* Ru(V)−OH moiety and a coherent rR band at 501 cm^{-1} (Figure 2b). DFT calculations (Table S1 and Figures S10−S11), performed on the whole system, provide the optimized geometry and indicate an open-shell doublet ground state for **2**, in accordance with the EPR observation (Inset in Figure 1).[17,18]

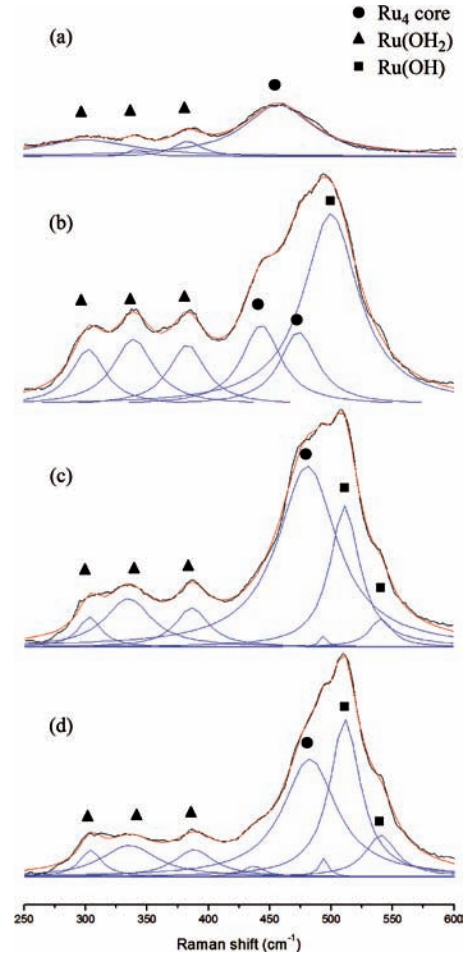

Figure 2. rR spectra (10^{-2} M in H_2O at pH = 0.6, 250−600 cm^{-1}, exciting line 488 nm) of (a) **1**, generated in situ upon reduction of **2** with 1 equiv of ascorbic acid; (b) **2**; (c and d) **2** upon addition of 1 and 2 equiv of Ce(IV), respectively.

Addition of 1 equiv of Ce(IV) to **2** yields an EPR silent species. Along the same line of reasoning, the formation of diamagnetic $[Ru^V_2(OH)_2Ru^{IV}_2(H_2O)_2(\mu\text{-}O)_4(\mu\text{-}OH)_2(\gamma\text{-}SiW_{10}O_{36})_2]^{10-}$, **3**, can account for the $\mathbf{S_2}$ state, where two of the four Ru(IV)−OH_2 are oxidized to Ru(V)−OH, with associated rR bands at 512 and 541 cm^{-1} (Figure 2c).[19]

Treatment of **2** with 2 equiv of Ce(IV) yields an EPR active system with composite features and a larger *g*-anisotropy in the spectral region expected for ruthenium species (Figure S14 in the Supporting Information).[20] The paramagnetic $\mathbf{S_3}$ state is then associated with $[Ru^V_3(OH)_3Ru^{IV}(H_2O)(\mu\text{-}O)_4(\mu\text{-}OH)_2(\gamma\text{-}SiW_{10}O_{36})_2]^{10-}$, **4**, displaying rR bands at 511 and 541 cm^{-1}, with a doublet ground state lying 2.1 kcal mol^{-1} below a quartet state. Thus, the building up of paramagnetic intermediates in alternate sequence, as predicted by computations and corresponding to the $\mathbf{S_1}$ and $\mathbf{S_3}$ states, is confirmed experimentally.

No variation of both the rR and the EPR spectra is registered upon further addition of Ce(IV), indicating that the high valent $\mathbf{S_4}$ intermediate is not observable under the conditions adopted.[21] The fate of **1** undergoing the overall $4e^-/4H^+$ loss has been addressed in silico. The formation of a Ru_4(V) complex, $[Ru^V_4(OH)_4(\mu\text{-}O)_4(\mu\text{-}OH)_2(\gamma\text{-}SiW_{10}O_{36})_2]^{10-}$, **5**, and of a mixed valent Ru_4{VI,VI,IV,IV} isoelectronic analogue, namely $[Ru^{VI}_2(O)_2Ru^{IV}_2(H_2O)_2(\mu\text{-}O)_4(\mu\text{-}OH)_2(\gamma\text{-}SiW_{10}O_{36})_2]^{10-}$, **6**, has been considered. Both **5** and **6** are predicted by DFT to have diamagnetic singlet ground states, as the triplet state for **5** is unstable and that for the **6** species is quasi-

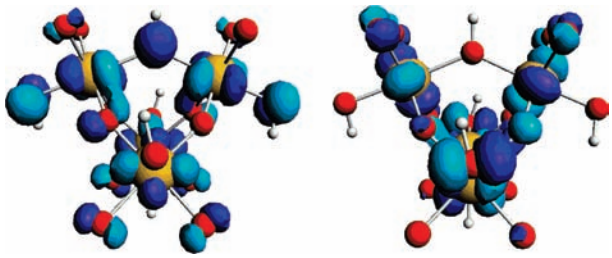

Figure 3. Plots of the quasi-degenerated LUMO (left) and LUMO+1 (right) of **5** (the POM ligand system is omitted for clarity).

degenerated. Noteworthy, **5** results in being energetically favored with respect to **6**.[22] The proposed structure of **5** contains four highly electrophilic $Ru^{V}(OH)$ moieties, prone to nucleophilic attack by an external water molecule. Plots of the quasi-degenerated LUMO and LUMO+1 Khon−Sham orbitals of **5** show a significant contribution of the terminal, Ru-bonded, OH sites (Figure 3).[23] The nucleophilic attack of water on the high valent ruthenium centers appears to be the only reasonable mode for O−O bond formation. Indeed, an intramolecular reaction between two adjacent ruthenium sites is herein neglected by geometrical constraints,[24,25] and alternative bimolecular pathways, involving two molecules of catalyst, are ruled out by first-order oxygen evolution kinetics.[9]

Such a mechanistic perspective foresees the formation of a peroxo-ruthenium intermediate, again in analogy with the enzymatic $\mathbf{S_4'}$ state,[26] which can finally release oxygen after a complex sequence of electron and proton transfer events.[27]

In conclusion, **1** is found to be a unique molecular catalyst for water oxidation, where the synergistic action of the four ruthenium sites sets forward an unprecedented bridge with the natural system.[28] At the same time it provides a functional paradigm to address some fundamental issues on oxygen−oxygen bond formation via a nucleophilic pathway, as delineated by convergent structural, kinetic, and computational evidence.

Acknowledgment. We thank Prof. Moreno Meneghetti (Nanophotonics Laboratory, University of Padova, Dept. of Chemical Sciences) for assistance with RAMAN spectroscopy and helpful discussions of data. Financial support from CNR, MIUR (FIRB CAMERE-RBNE03JCR5, PRIN Contract No. 2006034372), University of Padova (Progetto Strategico 2008, HELIOS, prot. STPD08RCX), the ESF COST D40 action, is gratefully acknowledged. P.M. wants to thank the Generalitat de Catalunya for an FI fellowship (2009FIC00026) and support by University and Research Commission of Innovation, University and Enterprise Department of Catalan Government and European Social Fund. We are indebted to the MICINN of the Spanish Government (Grants CTQ2007-67918/BQU, CTQ2008-06549-C02-02/BQU, and Consolider Ingenio 2010 CSD2006-0003), to the CIRIT of the Catalan Government (Grants 2009SGR69 and 2009SGR259), and to the ICIQ Foundation for financial support. The authors thankfully acknowledge the computer resources, technical expertise, and assistance provided by the Barcelona Supercomputing Center - Centro Nacional de Supercomputación.

Supporting Information Available: Electrochemistry, rRaman, EPR, UV−vis spectra and computational details. This material is available free of charge via the Internet at http://pubs.acs.org.

References

(1) (a) Que, L., Jr; Tolman, W. B. *Angew. Chem., Int. Ed.* **2002**, *41*, 1114–1137. (b) Que, L., Jr.; Tolman, W. B. *Nature* **2008**, *455*, 333–340.
(2) Ferreira, K. N.; Iverson, T. M.; Maghlaoui, K.; Barber, J.; Iwata, S. *Science* **2004**, *303*, 1831–1838.
(3) (a) Sproviero, E. M.; Gascon, J. A.; McEvoy, J. P.; Brudvig, G. W.; Batista, V. S. *Coord. Chem. Rev.* **2008**, *252*, 395–415. (b) Sauer, K.; Yano, J.; Yachandra, V. K. *Coord. Chem. Rev.* **2008**, *252*, 318–335.
(4) (a) Gray, H. B. *Nat. Chem.* **2009**, *1*, 7. (b) Eisenberg, R; Gray, H. B. *Inorg. Chem.* **2008**, *47*, 1697–1699. (c) Meyer, T. J. *Nature* **2008**, *451*, 778–779.
(5) (a) Lutterman, D. A.; Surendranath, Y.; Nocera, D. G. *J. Am. Chem. Soc.* **2009**, *131*, 3838–3839. (b) Kanan, M. W.; Nocera, D. G. *Science* **2008**, *321*, 1072–1075. (c) McDaniel, N. D.; Coughlin, F. J.; Tinker, L. L.; Bernhard, S. *J. Am. Chem. Soc.* **2008**, *130*, 210–217. (d) Tinker, L. L.; McDaniel, N. D.; Bernhard, S. *J. Mater. Chem.* **2009**, *19*, 3328–3337.
(6) Sala, X.; Romero, I.; Rodríguez, M.; Viñas, C.; Parella, T.; Llobet, A. *Angew. Chem., Int. Ed.* **2009**, *48*, 2842–2852.
(7) (a) Concepcion, J. J.; Jurss, J. W.; Templeton, J. L.; Meyer, T. J *Proc. Natl. Acad. Sci. U.S.A.* **2008**, *105*, 17632–17635. (b) Gersten, S. W.; Samuels, G. J.; Meyer, T. J. *J. Am. Chem. Soc.* **1982**, *104*, 4029–4030.
(8) Sens, C.; Romero, I.; Rodríguez, M.; Llobet, A.; Parella, T.; Benet-Bucholz, J. *J. Am. Chem. Soc.* **2004**, *126*, 7798–7799.
(9) Sartorel, A.; Carraro, M.; Scorrano, G.; De Zorzi, R.; Geremia, S.; McDaniel, N. D.; Bernhard, S.; Bonchio, M. *J. Am. Chem. Soc.* **2008**, *130*, 5006–5007.
(10) (a) Geletii, Y. V.; Botar, B.; Köegerler, P.; Hillesheim, D. A.; Musaev, D. G.; Hill, C. L. *Angew. Chem., Int. Ed.* **2008**, *47*, 3896–3899. (b) Geletii, Y. V.; Huang, Z.; Hou, Y.; Musaev, D. G.; Lian, T.; Hill, C. L. *J. Am. Chem. Soc.* **2009**, *131*, 7522–7523.
(11) Liu, F.; Concepcion, J. J.; Jurss, J. W.; Cardolaccia, T.; Templeton, J. L.; Meyer, T. J. *Inorg. Chem.* **2008**, *47*, 1727–1752.
(12) Romero, I.; Rodríguez, M.; Sens, C.; Mola, J.; Kollipara, M. R.; Francas, L.; Mas-Marza, E.; Esriche, L.; Llobet, A. *Inorg. Chem.* **2008**, *47*, 1824–1834.
(13) Large g anisotropy and $\langle g \rangle$ values significantly lower than the free electron value have been observed for paramagnetic intermediates of the ruthenium blue dimer (see ref 15). The sharp component with $g = 1.77$, although appearing as a prominent feature in the experimental spectrum, represents only a 10% contribution to the overall signal, as estimated by double integration.
(14) Lahootun, V.; Besson, C.; Villanneau, R.; Villain, F.; Chamoreau, L.-M.; Boubekeur, K.; Blanchard, S.; Thouvenot, R.; Proust, A. *J. Am. Chem. Soc.* **2007**, *129*, 7127–7135.
(15) Yamada, H.; Hurst, J. K. *J. Am. Chem. Soc.* **2000**, *122*, 5303–5311.
(16) Calculated Raman for $[Ru^{IV}_4(\mu\text{-}OH)_2(\mu\text{-}O)_4(H_2O)_4Cl_8]^{2-}$ shows two bands at 449 and 463 cm^{-1}, due to the core stretchings, and others at 295−302, 333, and 364−386 cm^{-1} due to Ru−OH_2 vibrations.
(17) The higher multiplicity state of **2** (quartet) is less stable by 3.0 kcal mol^{-1}. Calculated energies and geometric parameters reported in the paper refer to the gas phase. Single-point calculations including solvent effects do not show significant changes.
(18) The pK_a for the Ru(V)-hydroxo group in **2** was calculated by DFT to be 4.2, thus confirming the attribution of a protonated state at pH 0.6; see Supporting Information, Figure S15.
(19) Two isomeric structures for **3** can be considered: **3a**, where both Ru(V) centers are linked to the same $\mathbf{SiW_{10}}$ unit, and **3b**, where the two Ru(V) centers are bound to a different $\mathbf{SiW_{10}}$ unit. DFT calculations predict a triplet ground state for **3a** and **3b**, even if the open shell singlet energies are corrected, with **3b** being 1.9 kcal·mol^{-1} more stable than **3a**. Note that DFT methods are unable to properly describe open-shell singlet states; see: Ziegler, T.; Rauk, A.; Baerends, E. J. *Theor. Chim. Acta* **1977**, *43*, 261–271.
(20) The observed, complex line shape could be due to dipolar interactions between different molecules or to partial aggregation or precipitation phenomena at the cryogenic temperature of the experiment.
(21) rR and EPR monitoring of the stepwise oxidation of **1** has been performed by the *in situ* addition of increasing Ce(IV) equivalents, in water, with immediate freezing of the solutions at−50 °C. Such a procedure likely precludes the building up of a detectable concentration of the reactive $\mathbf{S_4}$ state.
(22) The energy difference was found in the range 9−17 kcal mol^{-1}, depending on the level of theory used; see Tables S1 and S2. In analogy with **3** (see ref 19), two structural isomers **6a** and **6b** have been considered, with **6b** being slightly more stable than **6a**.
(23) A similar scenario results for the two Ru(VI)-oxo functionalities in **6a** (Figure S16), where the LUMO+1 is mostly localized.
(24) Romain, S.; Bozoglian, F.; Sala, X.; Llobet, A. *J. Am. Chem. Soc.* **2009**, *131*, 2768–2769.
(25) Labelling experiments with H_2O^{18} as a probe of nucleophilic attack are hampered by fast equilibria exchange of water ligands at the Ru_4-core.
(26) McEvoy, J. P.; Brudvig, G. V. *Chem. Rev.* **2006**, *106*, 4455–4483.
(27) Alternative pathways, including the formation of hydrogen peroxide in solution, are currently under investigation. Catalase activity by **1** leading to dismutation of a H_2O_2 excess, forming water and O_2, has been observed in both acidic and neutral aqueous solutions.
(28) Few polynuclear Mn-based complexes have been reported to oxidize water to oxygen with low turnovers, but their activity is still debated, as in most cases peroxides have been used as the oxidant. See: Mullins, C. S.; Pecoraro, V. L. *Coord. Chem. Rev.* **2008**, *252*, 416–443.

JA905067U